

Attack is Good Augmentation: Towards Skeleton-Contrastive Representation Learning

Binqian Xu¹ Xiangbo Shu¹ Rui Yan² Guo-Sen Xie¹ Yixiao Ge³ Mike Zheng Shou⁴

¹Nanjing University of Science and Technology ²Nanjing University

³Tencent ⁴National University of Singapore

{xubinq11, yanrui6019, gsxiehm, geyixiao831, mike.zheng.shou}@gmail.com shuxb@njjust.edu.cn

Abstract

Contrastive learning, relying on effective positive and negative sample pairs, is beneficial to learn informative skeleton representations in unsupervised skeleton-based action recognition. To achieve these positive and negative pairs, existing weak/strong data augmentation methods have to randomly change the appearance of skeletons for indirectly pursuing semantic perturbations. However, such approaches have two limitations: 1) solely perturbing appearance cannot well capture the intrinsic semantic information of skeletons, and 2) randomly perturbation may change the original positive/negative pairs to soft positive/negative ones. To address the above dilemma, we start the first attempt to explore an attack-based augmentation scheme that additionally brings in direct semantic perturbation, for constructing hard positive pairs and further assisting in constructing hard negative pairs. In particular, we propose a novel Attack-Augmentation Mixing-Contrastive learning (A^2MC) to contrast hard positive features and hard negative features for learning more robust skeleton representations. In A^2MC , Attack-Augmentation (Att-Aug) is designed to collaboratively perform targeted and untargeted perturbations of skeletons via attack and augmentation respectively, for generating high-quality hard positive features. Meanwhile, Positive-Negative Mixer (PNM) is presented to mix hard positive features and negative features for generating hard negative features, which are adopted for updating the mixed memory banks. Extensive experiments on three public datasets demonstrate that A^2MC is competitive with the state-of-the-art methods.

1. Introduction

Human action recognition is a fundamental topic in the field of computer vision with various application scenarios, e.g. video surveillance, human-machine interaction, entertainment, etc. [2, 36, 38]. Due to the lightweight and

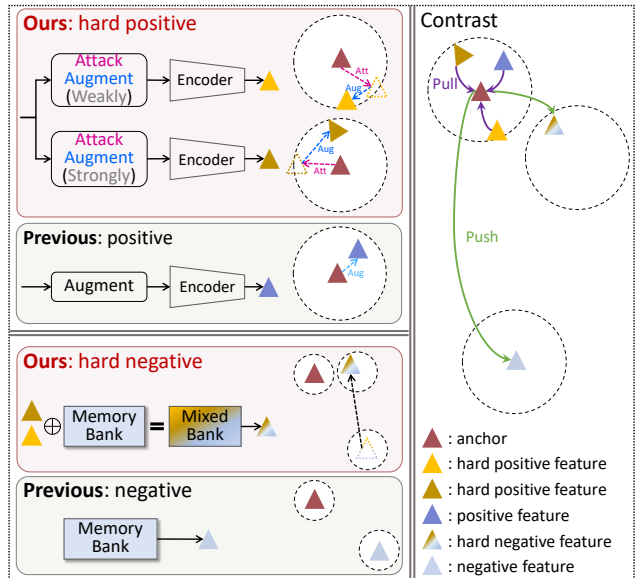


Figure 1: Main idea of this work. Previous weak/strong augmentations randomly construct positive features for the anchor while directly treating them as negative features in the memory bank. Our work introduces an attack-augmentation (“Att”: attack features for moving them toward the semantic boundary, and “Aug”: randomly augment features for diversity) to generate hard positive features, and further construct positive-negative mixed features as hard negative features. Compared with positive/negative features, our hard positive/negative features are more beneficial for contrastive learning.

robustness of skeletons, skeleton-based action recognition has attracted a lot of attention [15, 21, 37]. In recent years, supervised methods have achieved satisfactory performance, but the requirement for sufficient labeled data remains an obstacle [20, 48, 51]. Alternatively, many unsupervised methods in the field have emerged endlessly,

mainly based on the following three types of models, i.e., encoder-decoder [40, 56], contrastive learning [9, 19], and Transformer [6, 14]. Among them, contrastive learning-based methods are naturally specific for unsupervised tasks, and continue to be attractive in the community [5, 9, 14].

Generally, the process of contrastive learning is to pull the positive pairs closer and push the negative pairs away for learning representation of data [3, 11]. Therefore, the key to contrastive learning is to construct positive (similar) pairs and negative (dissimilar) pairs [10, 33]. In the unsupervised skeleton-based action recognition task, weak/strong augmentation is the most general way to construct positive and negative features [9, 19, 22], which always performs random appearance perturbation for indirectly realizing the semantic perturbation. However, solely perturbing the appearance of skeletons cannot well capture the intrinsic semantic information of skeletons, due to that the indirect semantic perturbation caused by appearance perturbation is not consistent with direct semantic perturbation. Besides, randomly perturbing appearance may change the original positive/negative pairs to soft positive/negative ones. Compared with soft positive/negative features, hard positive/negative features are more beneficial for contrastive learning. Intuitively, a desirable hard positive feature should be close to the semantic inner boundary of the anchor, namely it should be far away the anchor as far as possible. Similarly, a desirable hard negative feature should be close to the semantic outer boundary of the anchor [13, 33].

Thus, how to effectively move positive and negative features toward the semantic inner and outer boundaries of the anchor respectively is the key to constructing desirable hard positive pairs and hard negative pairs. Inspired by the White-box Attack [24, 46] at the semantic level, we start the first attempt to design an Attack-Augmentation (Att-Aug) mechanism equipped with weak/strong attack-augmentation to realize the direct semantic perturbation and appearance perturbation, for effectively generating hard positive features, and further assisting in constructing hard negative features. As shown in Figure 1, weak/strong attack-augmentation performs the semantic perturbation of skeleton by attacking the feature for being close to the semantic boundary, as well as performing the appearance perturbation for producing more diverse hard positive features. Subsequently, these hard positive features are further mixed with negative features from an updating memory bank to generate hard negative features, which are adopted for updating the mixed memory banks.

Based on Att-Aug, we propose a novel Attack-Augmentation Mixing-Contrastive learning (A^2MC) framework for unsupervised skeleton-based action recognition, as shown in Figure 2. Specifically, Attack-Augmentation (Att-Aug) mechanism is used to construct hard positive features, in which the skeletons are first updated by the attack loss to

get close to the semantic boundary, and then passed through weak/strong augmentations and query encoders to obtain abundant hard positive features. Then, Positive-Negative Mixer (PNM) mixes a small proportion of hard positive features and a large proportion of adversarial negative features (in a learnable memory bank) to generate hard negative features (in the mixed memory banks). Finally, Mixing Contrast (MC) loss trains the entire network by pulling similarity distribution closer to one-hot distribution or similarity distribution calculated from basic augmented features. Experiments on NTU RGB+D 60, NTU RGB+D 120, and PKU-MMD demonstrate the effectiveness of the proposed A^2MC on the unsupervised skeleton-based action recognition task. Overall, the main contributions of this work can be summarized as follows,

- We propose a novel Attack-Augmentation Mixing-Contrastive learning (A^2MC) framework that effectively constructs hard positive and negative pairs, enabling the model to learn more robust skeleton representations for unsupervised skeleton-based action recognition.
- To explore richer hard positive features, we design a new Attack-Augmentation (Att-Aug) mechanism that attacks and augments skeleton sequences mainly for the targeted semantic perturbation and untargeted appearance perturbation, respectively.
- To construct and update hard negative features, we present a new Positive-Negative Mixer (PNM) that mixes hard positive features and adversarial negative features, and then updates the mixed memory banks.

2. Related work

Unsupervised skeleton action recognition. Many unsupervised methods have emerged for skeleton-based action recognition that aim to learn representations from unlabeled data [5, 9, 14, 18, 19, 22, 27, 39, 40, 41, 42, 44, 45, 49, 50, 52, 53, 54]. Existing methods almost belong to three categories: encoder-decoder, contrastive learning, and Transformer. Since the emergence of MoCo [4, 11] in 2020, contrastive learning-based methods have been extensively studied. For example, Inter-skeleton Contrast (ISC) [44] is proposed to learn multiple different skeleton representations in an inter- and intra-contrastive manner. Beyond single-view contrastive learning, CrosSCLR [19] additionally explores cross-view contrast between joint and motion views. Recently, Cross-modal Mutual Distillation (CMD) [27] utilizes the k -nearest neighbors of the anchor in the memory bank for constructing more positive pairs, and explores the neighboring similarity distribution in the contrastive frameworks. In this work, the proposed A^2MC is also evolved

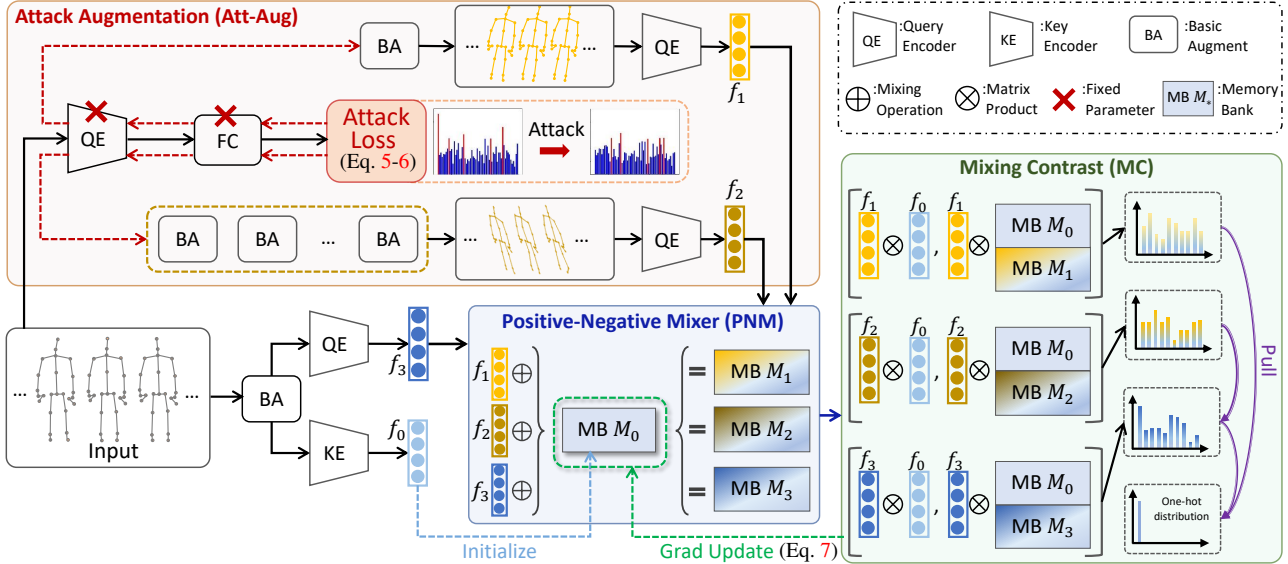


Figure 2: Framework of the proposed A²MC. Given the skeleton input, Att-Aug produces two types of attacked features f_1/f_2 (weak and strong versions) as hard positive features (§3.2), while features f_0/f_3 are obtained via basic augment and key/query encoder (§3.1). PNM mixes features $f_1/f_2/f_3$ and memory bank M_0 to generate mixed memory banks $M_1/M_2/M_3$, in which memory bank M_0 is an ensemble of adversarial negative features updated by gradient, initialized by features f_0 (§3.3). In MC, the similarity distributions calculated from f_1 and f_3 are respectively pulled to the one-hot distribution, and the similarity distribution calculated from f_2 is pulled to the similarity distribution calculated from f_3 (§3.4).

from MoCo by using the mixing memory bank instead of the traditional memory bank to address the problem of unsupervised skeleton-based action recognition.

Contrastive learning. Contrastive learning aims to learn data representation by measuring the similarity/dissimilarity on the constructed positive/negative pairs [3, 10, 11, 33]. Many methods consider different augmentation strategies to construct positive features for the anchor feature [3, 9, 22, 32, 44, 55]. Among them, ASCAL [32] utilizes seven different normal augmentations to produce the positive features, such as rotate, shear, reverse and so on. Besides the normal augmentations, AimCLR [9] combines eight augmentation strategies to produce an extreme augmentation to enrich diverse features. To alleviate the inconsistency caused by extreme augmentation, Zhang et al. [55] introduce a step-by-step hierarchical augmentation to construct more consistent positive pairs. Moreover, some studies prove that hard negative features are also important for learning robust representations on contrastive learning [13, 33]. Likewise, the hard positive pairs may be also important, which is almost ignored in this community. In this work, we explore the characteristic of hard positive features, and aim to simultaneously construct hard positive and negative features.

Gradient-based white-box attack. Deep learning models are still vulnerable to adversarial perturbations and attacks [43], even though they have achieved outstanding per-

formance. Therefore, various adversarial attacks have been explored [1, 8, 26]. Among them, White-box Attack is one of the most representative attacks, wherein all knowledge of the target model is known [1]. In the White-box attack family, the gradient-based attack is one of the mainstream technologies used to fool the model by ascending the gradient on the model loss surface [8]. Recently, a few works [24, 46] attempt to leverage the gradient-based attack to test the robustness of the learning model. In this work, we explore the gradient-based White-box Attack to generate hard positive features for further improving the robustness of contrastive representation.

3. Methodology

3.1. Preliminary

Given the skeleton sequence x , we first perform basic data augmentation [44] (including pose augmentation or joint jittering, and temporal crop-resize) on it to obtain two augmented versions x_0 and x_3 , following MoCo v2 [4]. Subsequently, x_0 and x_3 are input into the key encoder and query encoder to produce features f_0 and f_3 , respectively. A memory bank $M = \{m_i\}_{i=1}^K$ stores a lot of negative features from f_0 in a first-in-first-out way. InfoNCE loss [29]

is employed to train the whole contrastive network, i.e.,

$$\mathcal{L}_{in} = -\log \frac{\exp(f_3^\top f_0/\tau)}{\exp(f_3^\top f_0/\tau) + \sum_{i=1}^K \exp(f_3^\top m_i/\tau)} \quad (1)$$

where τ is the temperature hyper-parameter. Similar to [9], we can also convert the above InfoNCE loss into another version for later understanding. The first step is to calculate the similarity distribution of u and v as follows,

$$\psi(u, v) = \frac{\exp(u^\top v/\tau)}{\exp(u^\top v/\tau) + \sum_{i=1}^K \exp(u^\top m_i/\tau)} \quad (2)$$

Thus, another version of InfoNCE loss is expressed as

$$\mathcal{L}_{in} = -\mathbf{1} \cdot \log \psi(f_3, f_0) - \sum_{i=1}^K \mathbf{0} \cdot \log \psi(f_3, m_i) \quad (3)$$

where $\mathbf{1}$ and $\mathbf{0}$ are the element indicators in the one-hot distribution. To maintain the consistency of the features stored in the memory bank M , the key encoder is a momentum-updated version of the query encoder, as follows,

$$\theta_k \leftarrow \alpha \theta_k + (1 - \alpha) \theta_q \quad (4)$$

where α is momentum coefficient, and θ_k/θ_q represents the parameter sets of key/query encoder.

3.2. Attack-Augmentation (Att-Aug)

Many contrastive-based methods adopt weak/strong augmentations to generate positive pairs [9, 19, 22, 27, 32, 55], but rarely explore how to generate real hard positive pairs. Intuitively, hard positive pairs should be mostly closer to the semantic inner boundary, which can increase contrasting capability for learning more robust representations. Thus, to construct hard positive features, we design a new Attack-Augmentation (Att-Aug) mechanism based on gradient-based White-box Attack, which collaboratively performs the targeted semantic attack and untargeted appearance augmentation. Specifically, the former aims to move the skeleton features to the semantic boundary of the anchor, and the latter randomly moves skeleton features for making them diverse.

Targeted semantic attack. For the skeleton sequence x , the attack aims to push its semantic feature to the semantic boundary in this work. First, x is input into a fixed query encoder and a fully-connected layer in turn to obtain its class feature $f_a \in \mathcal{R}^{C \times 1}$. Second, we formulate an attack loss to smooth f_a for moving the distribution of f_a towards a uniform distribution, so that the attacked \hat{x} is relatively closer to the semantic boundary compared with the original itself (anchor). Formally, the attack loss is formulated to maximize the entropy of f_a , as follows,

$$\begin{aligned} \mathcal{L}_{at} &= -\text{Entropy}(f_a) \\ &= \text{MSE}(f_a - \frac{1}{C} \mathbf{1}) \end{aligned} \quad (5)$$

where $\text{MSE}(\cdot)$ denotes the mean square error function, and $\mathbf{1}$ is an all-ones vector. After the attack loss is computed, the gradient of x is $\frac{\partial \mathcal{L}_{at}}{\partial x}$ for updating the skeleton sequence. And the attacked skeleton sequence \hat{x} is calculated as

$$\begin{aligned} \rho &= \epsilon \Phi\left(\frac{\partial \mathcal{L}_{at}}{\partial x}, x\right) \\ \hat{x} &= x + \rho, \quad \|\rho\|_2 < \eta \end{aligned} \quad (6)$$

where ϵ is the learning rate, Φ is Adam optimizer [16] to compute the updates, ρ denotes the perturbation restricted by ℓ_2 -norm, and η is a scalar value to ensure a certain imperceptibility in skeletons. So far, the skeleton sequence is closer to the semantic boundary of the anchor in the semantic space after the targeted semantic attack.

Untargeted appearance augmentation. Given the attacked skeleton sequence \hat{x} , weak and strong augmentations are performed on it to change its appearance, respectively. Specifically, the weak augmentation is consistent with the basic augmentation of contrastive learning, including pose augmentation or joint jittering, and temporal crop-resize. The strong augmentation consists of more basic augmentations [9]: pose augmentation or joint jittering, temporal crop-resize, spatial flip, rotate, gaussian noise, gaussian filter, and axis mask. Subsequently, weak/strong augmented skeleton sequences are converted to hard positive features f_1/f_2 via query encoders.

3.3. Positive-Negative Mixer (PNM)

It is learned from some studies that hard negative features can also increase contrasting capability [13, 33]. In this work, Positive-Negative Mixer (PNM) aims to mix negative features from an online updating memory bank and positive features ($f_1/f_2/f_3$) according to different weights, and further generate hard negative features participating in the updating of the mixed memory bank, which is detailed in the following.

Gradient-updating memory bank. Different from the traditional memory bank of basic contrastive learning in a first-in-first-out partial updating way, the memory bank M_0 of PNM as a whole is updated in the direction closer to the anchor by the gradient [12, 31]. First, M_0 is initialized by storing features from the key encoder. Suppose the total loss is calculated as \mathcal{L} after the forward propagation, the gradient respect to M_0 can be denoted as $\frac{\partial \mathcal{L}}{\partial M_0}$. Subsequently, the updating process of M_0 is expressed as follows,

$$M_0 \leftarrow M_0 + \beta \frac{\partial \mathcal{L}}{\partial M_0} \quad (7)$$

where β is the learning rate.

Positive-negative mixing. To further generate hard negative features based on M_0 , the strategy of mixing positive and negative features online is adopted. Specifically, given

the positive features (f_1 , f_2 , and f_3) and negative features from M_0 , the mixing process for generating memory banks M_1 , M_2 , and M_3 is calculated as follows,

$$M_* = \{m_{*i}\}_{i=1}^K = \{\lambda f_* + (1 - \lambda)m_{0i}\}_{i=1}^K \quad (8)$$

where the subscript $* \in \{1, 2, 3\}$, and λ is a mixing coefficient. Here, due to the import of the semantic of hard positive features, the generated hard negative features is relatively close to the semantic outer boundary of the anchor.

3.4. Mixing Contrast (MC)

In this work, Mixing Contrast (MC) loss is leveraged to contrast all positive and negative features, which pulls the similarity distributions among positive and negative features closer to the corresponding distributions, as shown in Figure 2. Formally, given all types of positive features $\{f_0, f_1, f_2, f_3\}$, and memory banks $\{M_0, M_1, M_2, M_3\}$, MC loss \mathcal{L} is defined as the final contrastive loss, i.e.,

$$\mathcal{L} = \mathcal{L}_1 + \mathcal{L}_2 + \mathcal{L}_3 \quad (9)$$

In \mathcal{L}_1 , the similarity distribution of f_0 , f_1 , M_0 , and M_1 is pulled toward the one-hot distribution. M_0 and M_1 are concatenated to generate the final memory bank M_{01} , and then \mathcal{L}_1 is calculated as follows,

$$\begin{aligned} M_{01} &= M_0 \cup M_1 = \{m_i\}_{i=1}^{2K} \\ \mathcal{L}_1 &= -\mathbf{1} \cdot \log \psi(f_1, f_0) - \sum_{i=1}^{2K} \mathbf{0} \cdot \log \psi(f_1, m_i) \end{aligned} \quad (10)$$

The calculation of \mathcal{L}_3 is the same as to \mathcal{L}_1 . Different from the above pulling of one-hot distribution, \mathcal{L}_2 needs to pull the similarity distribution of f_0 , f_2 , M_0 , and M_2 toward the similarity distribution from basic augmentation, due to the strong augmentation [9], as follows,

$$\begin{aligned} M_{02} &= M_0 \cup M_2 = \{m_i\}_{i=1}^{2K} \\ \mathcal{L}_2 &= -\psi(f_3, f_0) \cdot \log \psi(f_2, f_0) \\ &\quad - \sum_{i=1}^{2K} \psi(f_3, m_i) \cdot \log \psi(f_2, m_i) \end{aligned} \quad (11)$$

Finally, MC loss \mathcal{L} in Eq. (9) is used to train the whole framework of A²MC.

4. Experiments

4.1. Datasets

NTU RGB+D 60 (NTU-60) [34]: contains 56,880 skeleton sequences in 60 classes collected from 40 subjects by three cameras. In x-sub benchmark, training sets come from 20 subjects while testing sets come from the other 20 subjects. In x-view benchmark, training sets come from camera 2 and 3 while testing sets come from camera 1.

NTU RGB+D 120 (NTU-120) [25]: contains 114,480 skeleton sequences in 120 classes collected from 106 subjects with 32 setups, extended from NTU RGB+D 60. In x-sub benchmark, training sets come from 53 subjects while testing sets come from the other 53 subjects. In x-set benchmark, training sets come from even-numbered setups while testing sets come from odd-numbered setups.

PKU-MMD [23]: contains nearly 20,000 action clips in 51 classes, and consists of Phase I and Phase II (PKU-II) collected from Kinect cameras. PKU-II is more challenging due to the large view variation, which is recommended to validate the model. PKU-II contains 6,945 skeleton sequences in 41 action classes, performed by 13 subjects. In the recommended cross-subject benchmark, the training sets and testing sets include 5,332 and 1,613 skeleton sequences, respectively.

4.2. Implementation Details and Evaluation

Following the previous related works [27, 44], BiGRU is adopted as the encoder for a fair comparison. All sequence lengths are resized to the fixed 64 frames via temporal crop-resize [44]. We adopt SGD with momentum 0.9 and weight decay 10^{-4} to optimize the proposed A²MC. The initial learning rate and the mini-batch size are set to 0.01 and 64, respectively. All experiments are performed on the PyTorch framework [30].

Self-supervised Pre-training. In the contrastive learning based on MoCo v2 [4], the size of memory bank K , the temperature hyper-parameter τ , and momentum coefficient α are set to 16,384, 0.07, and 0.999, respectively. On NTU-60 and NTU-120, A²MC is pre-trained for 750 total epochs, and the learning rate drops to 0.001 after 350 epochs. On PKU-II, A²MC is pre-trained for 1,000 total epochs, and the learning rate drops to 0.001 after 800 epochs. In Att-Aug, the learning rate ϵ and the scalar value η are set to 0.1 and 0.5 for the one-step gradient-based White-box Attack. For the learnable memory bank M_0 of PNM, the learning rate β is 3.0 with a lower temperate of 0.03. To obtain more hard negative features, different mixing coefficients ($\lambda = 0.4, 0.3, 0.2, 0.1$) are set for pre-training.

Linear Evaluation. A learnable linear classifier is attached to the frozen query encoder to predict action classes. The whole network is trained for total 80 epochs with an initial learning rate of 0.1 (drops to 0.01 and 0.001 at epoch 50 and 70, respectively).

KNN Evaluation. A K-Nearest Neighbor (KNN) classifier is directly used to classify test samples without training, based on the K-nearest neighbor of features of the training samples learned by the query encoder, following [40].

Semi-supervised Evaluation. The query encoder first completes the pre-training contrastive task on all unlabeled data. Then, the pre-trained encoder and linear classifier are fine-tuned on randomly sampled 1% and 10% labeled data

Method	Type	Encoder	Params	NTU-60		NTU-120		PKU-II
				x-sub	x-view	x-sub	x-set	x-sub
MS ² L [22] (ACM MM 20)	hybrid	GRU	2.28M	52.6	-	-	-	27.6
PCRP [49] (IEEE TMM 21)	hybrid	GRU	-	54.9	63.4	43.0	44.6	-
LongT GAN [56] (AAAI 18)	Encoder decoder	GRU	40.2M	39.1	48.1	-	-	26.0
EnGAN [17] (WACV 19)	Encoder decoder	LSTM	-	68.6	77.8	-	-	-
P&C [40] (CVPR 20)	Encoder decoder	GRU	-	50.7	76.3	42.7	41.7	25.5
SeBiReNet [28] (ECCV 20)	Encoder decoder	GRU	0.27M	-	79.7	-	-	-
TS Colorization [52] (ICCV 21)	Encoder decoder	GCN	-	71.6	79.9	-	-	-
H-Transformer [6] (ICME 21)	Encoder decoder	Transformer	>100M	69.3	72.8	-	-	-
GL-Transformer [14] (ECCV 22)	Encoder decoder	Transformer	214M	76.3	83.8	66.0	68.7	-
AS-CAL [32] (INS 21)	Contrastive learning	LSTM	0.43M	58.5	64.8	48.6	49.2	-
ISC [44] (ACM MM 21)	Contrastive learning	GRU&CNN&GCN	10.0M	76.3	85.2	67.1	67.9	36.0
CrosSCLR [19] (CVPR 21)	Contrastive learning	GCN	0.85M	72.9	79.9	-	-	-
CrosSCLR-B [19] (CVPR 21)	Contrastive learning	BiGRU	10.0M	77.3	85.1	67.1	68.6	41.9
CRRL [47] (IEEE TIP 22)	Contrastive learning	LSTM	-	67.6	73.8	56.2	57.0	-
AimCLR [9] (AAAI 22)	Contrastive learning	GCN	0.85M	74.3	79.7	-	-	-
CPM [54] (ECCV 22)	Contrastive learning	GCN	3.4M	78.7	84.9	68.7	69.6	48.3
CMD [27] (ECCV 22)	Contrastive learning	BiGRU	10.0M	79.8	86.9	70.3	71.5	43.0
A ² MC (Ours)	Contrastive learning	BiGRU	10.0M	80.0	87.9	71.4	73.2	48.4

Table 1: Linear evaluation results on NTU-60, NTU-120, and PKU-II. CrosSCLR-B is reproduced in [27] by using BiGRU instead of GCN as the encoder. CMD, CrosSCLR, and CrosSCLR-B use multi-modality data, while the other methods only use single-modality data in the pre-training phase.

Method	Modality	x-sub
A ² MC	Joint	80.0
A ² MC	Motion	77.1
A ² MC	Bone	78.3
3s-CrosSCLR [19]	Joint+Motion+Bone	77.8
3s-AimCLR [9]	Joint+Motion+Bone	78.9
3s-HiCLR [55]	Joint+Motion+Bone	80.4
3s-CrosSCLR-B [19]	Joint+Motion+Bone	82.1
3s-CPM [54]	Joint+Motion+Bone	83.2
3s-HiCo [7]	Joint+Motion+Bone	83.8
3s-CMD [27]	Joint+Motion+Bone	84.1
3s-A ² MC	Joint+Motion+Bone	84.6

Table 2: Linear evaluation results in different modalities on NTU-60.

for 80 epochs with an initial learning rate of 0.01 (drops to 0.001 and 0.0001 at epoch 50 and 70).

Transfer Learning Evaluation. The query encoder is first pre-trained on the source dataset, and then fine-tuned together with the linear classifier on the target dataset for 80 epochs with an initial learning rate of 0.01 (drops to 0.001 and 0.0001 at epoch 50 and 70). Here, the source dataset is the training set from NTU-60/NTU-120 (x-sub), while the target dataset is the testing set from PKU-II.

4.3. Comparison with State-of-the-arts

Linear Evaluation Results. As shown in Table 1, the proposed A²MC achieves the best performance compared with other related works. Notably, whether the encoder is Transformer, GCN, or BiGRU, A²MC is competitive with the alternatives. Specifically, with the consistent BiGRU configuration, A²MC outperforms the corresponding SOTA method (i.e., CMD [27]) by 1.7% and 5.4% on NTU-120 (x-set) and PKU-II (x-sub). Here, CMD mines positive pairs among existing negative pairs based on the neighboring similarity distributions, while A²MC constructs new hard positive features by attacking and augmenting skeletons. With the same GCN (i.e., ST-GCN [51]) configuration, A²MC is comparable to CPM [54]. The former considers the semantic-attacked itself as the hard positive feature, while the latter identifies others in a contextual queue as the hard positive ones. With Transformer (i.e., DSTA-Net [35]) as encoder, A²MC also achieves better performance with fewer parameters compared to Transformer-based SOTA method, i.e., GL-Transformer [14].

We also conduct comparative experiments to evaluate the performance of A²MC using the three-modality data (including joint, motion, and bone) as input on NTU-60 (x-sub). For multi-modal skeleton sequences with joint, motion, and bone, we simply extend A²MC to a three-stream version, i.e., 3s-A²MC, without any elaborate design. As shown in Table 2, 3s-A²MC achieves comparable performance to that of 3s-CMD [27], which is the SOTA method

Method	NTU-60		NTU-120	
	x-sub	x-view	x-sub	x-set
LongT GAN [56]	39.1	48.1	31.5	35.5
P&C [40]	50.7	76.3	39.5	41.8
ISC [44]	62.5	82.6	50.6	52.3
CrosSCLR-B [19]	66.1	81.3	52.5	54.9
HiCLR [55]	67.3	75.3	-	-
HiCo [7]	68.3	84.8	56.6	59.1
CMD [27]	70.6	85.4	58.3	60.9
A ² MC (Ours)	70.8	85.4	59.1	62.6

Table 3: KNN evaluation results on NTU-60, and NTU-120.

Method	x-sub		x-view	
	1%	10%	1%	10%
	LongT GAN [56]	35.2	62.0	-
MS ² L [22]	33.1	65.2	-	-
ASSL [39]	-	64.3	-	69.8
ISC [44]	35.7	65.9	38.1	72.5
CrosSCLR-B [19]	48.6	72.4	49.8	77.0
CMD [27]	50.6	75.4	53.0	80.2
A ² MC (Ours)	52.0	76.4	53.5	81.5

Table 4: Semi-supervised evaluation results on NTU-60.

designed for specifically handling multiple modalities.

KNN Evaluation Results. KNN Evaluation is also regarded as the action retrieval task in some previous works [7, 44]. From the KNN evaluation results in Table 3, A²MC outperforms the SOTA method (i.e., CMD [27]) by 1.7% on NTU-120, and it is comparable to CMD on NTU-60. It demonstrates that A²MC can learn high-quality features in the discriminative space in an unsupervised way.

Semi-supervised Evaluation Results. To verify the performance of A²MC in the semi-supervised scenario, we conduct experiments on NTU-60 with a small amount of labeled data. As shown in Table 4, A²MC outperforms CMD [27] by 1.4% and 1.3% on x-sub with 1% labeled data and x-view with 10% labeled data, respectively.

Transfer Learning Evaluation Results. We conduct experiments to test whether the knowledge learned from the source dataset is helpful for learning on the target dataset, i.e., whether the learned features are generalizable. The transfer learning evaluation results are shown in Table 5. Compared with other methods, the features learned by A²MC show better generalization, especially with 2.1% higher performance than CMD [27] when transferring from NTU-60 (x-sub) to PKU-II.

4.4. Ablation Study

Effectiveness of different components. To demonstrate the effectiveness of different components (including Att-Aug, PNM, and MC Loss) in the A²MC framework, we

Method	Transfer to PKU-II	
	NTU-60 (x-sub)	NTU-120 (x-sub)
LongT GAN [56]	44.8	-
MS ² L [22]	45.8	-
ISC [44]	51.1	52.3
CrosSCLR-B [19]	54.0	52.8
CMD [27]	56.0	57.0
A ² MC (Ours)	58.1	58.9

Table 5: Transfer learning evaluation results.

Baseline	Att-Aug	PNM	MC	NTU-60	
				x-sub	x-view
B1	✗	✗	✗	75.6	82.8
B2	✓	✗	✗	78.5	85.6
B3	✓	✗	✓	79.0	86.7
A ² MC	✓	✓	✓	80.0	87.9

Table 6: Ablation study under linear evaluation on NTU-60.

conduct the ablation study for different components on NTU-60, as shown in Table 6. Based on B1 (basic contrastive learning with basic augmentations and InfoNCE loss), B2 (adding Att-Aug) improves performance by 2.9% and 2.8% on x-sub and x-view, proving the superiority of Att-Aug. By replacing InfoNCE loss with MC Loss in B3, the performance is further improved. The difference between InfoNCE loss and MC Loss is that the latter pulls the feature distribution toward the similarity distribution calculated from positive features instead of the one-hot distribution. Finally, by adding PNM based on B3, A²MC achieves the best performance that shows the effectiveness of PNM.

Visualization of Attack-Augmentation. To intuitively illustrate the different effects of Attack-Augmentation (Att-Aug) at the semantic and appearance levels, we visualize the feature distributions and skeletons before and after the attack, weak attack-augmentation, and strong attack-augmentation, as shown in Figure 3. From the perspective of the semantic level, the feature distribution after attack becomes smoother (refer to Top-5 bars) than before, while the results caused by weak/strong attack-augmentation have slight uncertainty. From the perspective of the appearance level, the changes of skeletons after attack are negligible, and the changes after strong attack-augmentation are relatively more obvious than those after weak attack-augmentation, which can further enrich representations with diverse appearance changes.

The t-SNE Visualization of features. We employ t-SNE algorithm to visualize the learned skeleton representations of A²MC compared with those of three baselines, including A²MC with only weak augmentation, A²MC with only weak and strong augmentations, A²MC with only attack.

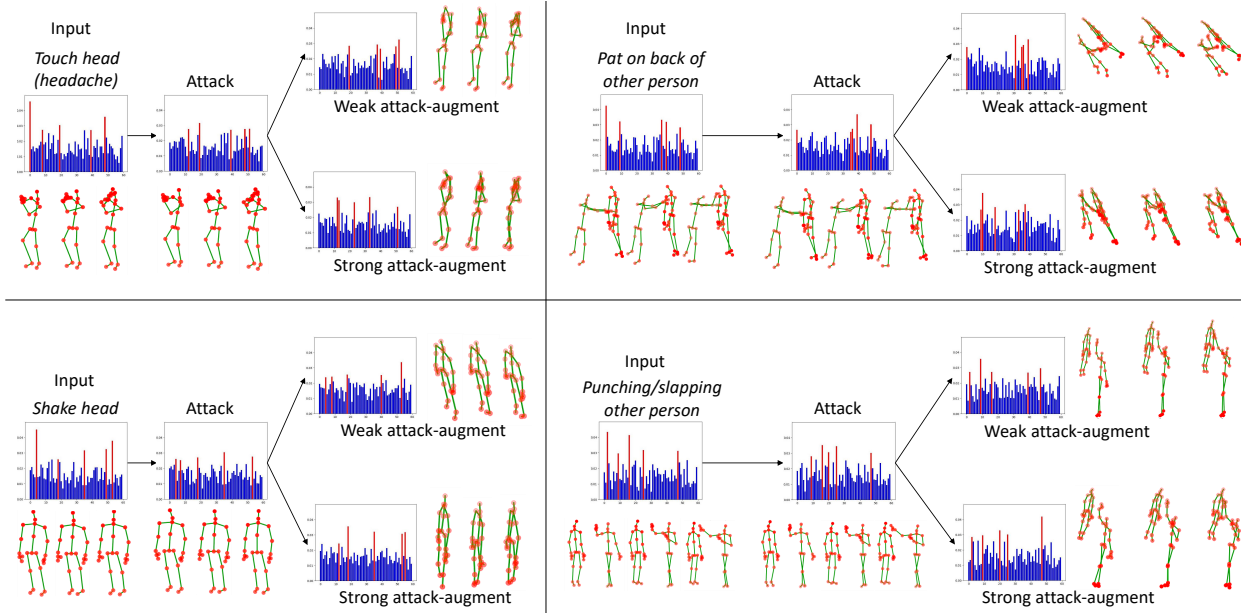


Figure 3: Visualization of attack-augmentation on NTU-60. For each group, given the original skeleton sequence, its skeletons and feature distributions after attack, weak attack-augmentation, and strong attack-augmentation are respectively visualized. Here, we utilize FC layer to obtain the feature distribution, where Top-5 bars are highlighted.

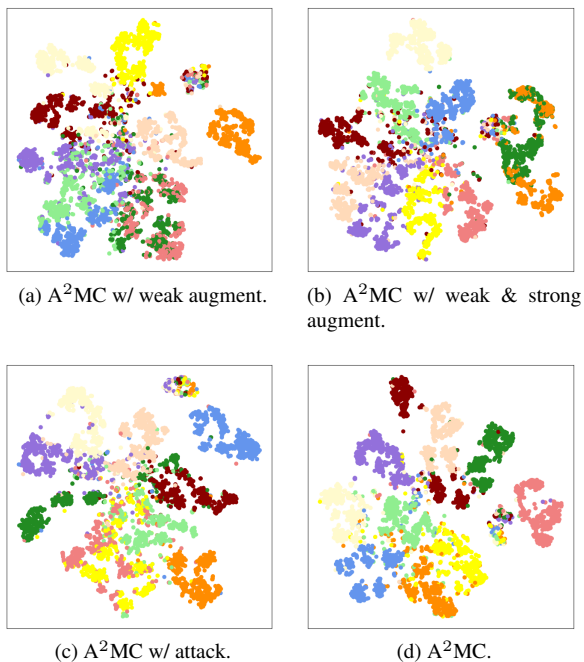


Figure 4: The t-SNE visualization of features on NTU-60. Ten action classes are randomly selected and reported.

As shown in Figure 4, compared with such three baselines, the features learned by A²MC are more aggregated in

the same class and more discriminative in different classes, proving its representation learning capability.

5. Discussion

“A villain is an angel”. Attack is an angel we need in this work. The designed Attack-Augmentation (Att-Aug) is the first attempt to construct hard positive features by combining the advantages of attack and augmentation. The former perturbs the skeleton sequence mainly at the semantic level with the purpose of obtaining the features being close to the semantic boundary, while the latter perturbs the skeleton sequence mainly at the appearance level for randomly obtaining the diverse features. Specifically, to achieve such attacked result, we adopt the attack loss in an unsupervised way to smooth the feature distribution, in which the difference of top-k bars is suppressed to some extent. This is a simple yet effective way, even though there are various attack strategies that can also realize this purpose.

6. Conclusion

We propose a novel Attack-Augmentation Mixing-Contrastive learning (A²MC) framework for unsupervised skeleton-based action recognition. It integrates Attack-Augmentation (Att-Aug) mechanism and Positive-Negative Mixer (PNM) to generate hard positive/negative features for Mixing Contrast (MC). In particular, Att-Aug collaboratively implements targeted semantic attack and untar-

geted appearance augmentation of skeletons to facilitate the model to learn more robust representations. Extensive experiments demonstrate the superiority of A²MC. As the first attempt, our attack in A²MC is relatively straightforward, unlike the augmentation family within various weak/strong versions. This inspires us to further explore more attack-combination strategies in the future.

References

- [1] Naveed Akhtar, Ajmal Mian, Navid Kardan, and Mubarak Shah. Advances in adversarial attacks and defenses in computer vision: A survey. *IEEE Access*, 9:155161–155196, 2021. [3](#)
- [2] Joao Carreira and Andrew Zisserman. Quo vadis, action recognition? a new model and the kinetics dataset. In *CVPR*, 2017. [1](#)
- [3] Ting Chen, Simon Kornblith, Mohammad Norouzi, and Geoffrey Hinton. A simple framework for contrastive learning of visual representations. In *ICML*, 2020. [2, 3](#)
- [4] Xinlei Chen, Haoqi Fan, Ross Girshick, and Kaiming He. Improved baselines with momentum contrastive learning. *arXiv*, 2020. [2, 3, 5](#)
- [5] Yuxiao Chen, Long Zhao, Jianbo Yuan, Yu Tian, Zhaoyang Xia, Shijie Geng, Ligong Han, and Dimitris N Metaxas. Hierarchically self-supervised transformer for human skeleton representation learning. In *ECCV*, 2022. [2](#)
- [6] Yi-Bin Cheng, Xipeng Chen, Junhong Chen, Pengxu Wei, Dongyu Zhang, and Liang Lin. Hierarchical transformer: Unsupervised representation learning for skeleton-based human action recognition. In *ICME*, 2021. [2, 6](#)
- [7] Jianfeng Dong, Shengkai Sun, Zhonglin Liu, Shujie Chen, Baolong Liu, and Xun Wang. Hierarchical contrast for unsupervised skeleton-based action representation learning. *arXiv*, 2022. [6, 7](#)
- [8] Ian J Goodfellow, Jonathon Shlens, and Christian Szegedy. Explaining and harnessing adversarial examples. *arXiv*, 2014. [3](#)
- [9] Tianyu Guo, Hong Liu, Zhan Chen, Mengyuan Liu, Tao Wang, and Runwei Ding. Contrastive learning from extremely augmented skeleton sequences for self-supervised action recognition. In *AAAI*, 2022. [2, 3, 4, 5, 6](#)
- [10] Michael Gutmann and Aapo Hyvärinen. Noise-contrastive estimation: A new estimation principle for unnormalized statistical models. In *AISTATS*, 2010. [2, 3](#)
- [11] Kaiming He, Haoqi Fan, Yuxin Wu, Saining Xie, and Ross Girshick. Momentum contrast for unsupervised visual representation learning. In *CVPR*, 2020. [2, 3](#)
- [12] Qianjiang Hu, Xiao Wang, Wei Hu, and Guo-Jun Qi. Adco: Adversarial contrast for efficient learning of unsupervised representations from self-trained negative adversaries. In *CVPR*, 2021. [4](#)
- [13] Yannis Kalantidis, Mert Bulent Sariyildiz, Noe Pion, Philippe Weinzaepfel, and Diane Larlus. Hard negative mixing for contrastive learning. In *NeurIPS*, 2020. [2, 3, 4](#)
- [14] Boeun Kim, Hyung Jin Chang, Jungho Kim, and Jin Young Choi. Global-local motion transformer for unsupervised skeleton-based action learning. In *ECCV*, 2022. [2, 6](#)
- [15] Tae Soo Kim and Austin Reiter. Interpretable 3d human action analysis with temporal convolutional networks. In *CVPR Workshops*, 2017. [1](#)
- [16] Diederik P Kingma and Jimmy Ba. Adam: A method for stochastic optimization. *arXiv*, 2014. [4](#)
- [17] Jogendra Nath Kundu, Maharshi Gor, Phani Krishna Uppala, and Venkatesh Babu Radhakrishnan. Unsupervised feature learning of human actions as trajectories in pose embedding manifold. In *WACV*, 2019. [6](#)
- [18] Jingyuan Li and Eli Shlizerman. Sparse semi-supervised action recognition with active learning. *arXiv*, 2020. [2](#)
- [19] Linguo Li, Minsi Wang, Bingbing Ni, Hang Wang, Jiancheng Yang, and Wenjun Zhang. 3d human action representation learning via cross-view consistency pursuit. In *CVPR*, 2021. [2, 4, 6, 7](#)
- [20] Maosen Li, Siheng Chen, Xu Chen, Ya Zhang, Yanfeng Wang, and Qi Tian. Actional-structural graph convolutional networks for skeleton-based action recognition. In *CVPR*, 2019. [1](#)
- [21] Shuai Li, Wanqing Li, Chris Cook, Ce Zhu, and Yanbo Gao. Independently recurrent neural network (indrnn): Building a longer and deeper rnn. In *CVPR*, 2018. [1](#)
- [22] Lilang Lin, Sijie Song, Wenhan Yang, and Jiaying Liu. Ms2l: Multi-task self-supervised learning for skeleton based action recognition. In *ACM MM*, 2020. [2, 3, 4, 6, 7](#)
- [23] Chunhui Liu, Yueyu Hu, Yanghao Li, Sijie Song, and Jiaying Liu. Pku-mmd: A large scale benchmark for continuous multi-modal human action understanding. *arXiv*, 2017. [5](#)
- [24] Jian Liu, Naveed Akhtar, and Ajmal Mian. Adversarial attack on skeleton-based human action recognition. *IEEE TNNLS*, 33(4):1609–1622, 2020. [2, 3](#)
- [25] Jun Liu, Amir Shahroudy, Mauricio Perez, Gang Wang, Ling-Yu Duan, and Alex C Kot. Ntu rgb+ d 120: A large-scale benchmark for 3d human activity understanding. *IEEE TPAMI*, 42(10):2684–2701, 2019. [5](#)
- [26] Aleksander Madry, Aleksandar Makelev, Ludwig Schmidt, Dimitris Tsipras, and Adrian Vladu. Towards deep learning models resistant to adversarial attacks. *arXiv*, 2017. [3](#)
- [27] Yunyao Mao, Wengang Zhou, Zhenbo Lu, Jiajun Deng, and Houqiang Li. Cmd: Self-supervised 3d action representation learning with cross-modal mutual distillation. In *ECCV*, 2022. [2, 4, 5, 6, 7](#)
- [28] Qiang Nie, Ziwei Liu, and Yunhui Liu. Unsupervised 3d human pose representation with viewpoint and pose disentanglement. In *ECCV*, 2020. [6](#)
- [29] Aaron van den Oord, Yazhe Li, and Oriol Vinyals. Representation learning with contrastive predictive coding. *arXiv*, 2018. [3](#)
- [30] Adam Paszke, Sam Gross, Soumith Chintala, Gregory Chanan, Edward Yang, Zachary DeVito, Zeming Lin, Alban Desmaison, Luca Antiga, and Adam Lerer. Automatic differentiation in pytorch. In *NeurIPS Workshops*, 2017. [5](#)
- [31] Guo-Jun Qi and Mubarak Shah. Adversarial pretraining of self-supervised deep networks: Past, present and future. *arXiv*, 2022. [4](#)
- [32] Haocong Rao, Shihao Xu, Xiping Hu, Jun Cheng, and Bin Hu. Augmented skeleton based contrastive action learning

- with momentum lstm for unsupervised action recognition. *Information Sciences*, 569:90–109, 2021. 3, 4, 6
- [33] Joshua Robinson, Ching-Yao Chuang, Suvrit Sra, and Stefanie Jegelka. Contrastive learning with hard negative samples. *arXiv*, 2020. 2, 3, 4
- [34] Amir Shahroudy, Jun Liu, Tian-Tsong Ng, and Gang Wang. Ntu rgb+d: A large scale dataset for 3d human activity analysis. In *CVPR*, 2016. 5
- [35] Lei Shi, Yifan Zhang, Jian Cheng, and Hanqing Lu. Decoupled spatial-temporal attention network for skeleton-based action-gesture recognition. In *ACCV*, 2020. 6
- [36] Xiangbo Shu, Jinhui Tang, Guojun Qi, Wei Liu, and Jian Yang. Hierarchical long short-term concurrent memory for human interaction recognition. *IEEE TPAMI*, 40(3):1110–1118, 2021. 1
- [37] Xiangbo Shu, Liyan Zhang, Guo-Jun Qi, Wei Liu, and Jinhui Tang. Spatiotemporal co-attention recurrent neural networks for human-skeleton motion prediction. *IEEE TPAMI*, 44(6):3300–3315, 2021. 1
- [38] Xiangbo Shu, Liyan Zhang, Yunlian Sun, and Jinhui Tang. Host-parasite: Graph lstm-in-lstm for group activity recognition. *IEEE TNNLS*, 32(2):663–674, 2021. 1
- [39] Chenyang Si, Xuecheng Nie, Wei Wang, Liang Wang, Tieniu Tan, and Jiashi Feng. Adversarial self-supervised learning for semi-supervised 3d action recognition. In *ECCV*, 2020. 2, 7
- [40] Kun Su, Xiulong Liu, and Eli Shlizerman. Predict & cluster: Unsupervised skeleton based action recognition. In *CVPR*, 2020. 2, 5, 6, 7
- [41] Yukun Su, Guosheng Lin, Ruizhou Sun, Yun Hao, and Qingyao Wu. Modeling the uncertainty for self-supervised 3d skeleton action representation learning. In *ACM MM*, 2021. 2
- [42] Yukun Su, Guosheng Lin, and Qingyao Wu. Self-supervised 3d skeleton action representation learning with motion consistency and continuity. In *ICCV*, 2021. 2
- [43] Christian Szegedy, Wojciech Zaremba, Ilya Sutskever, Joan Bruna, Dumitru Erhan, Ian Goodfellow, and Rob Fergus. Intriguing properties of neural networks. *arXiv*, 2013. 3
- [44] Fida Mohammad Thoker, Hazel Doughty, and Cees GM Snoek. Skeleton-contrastive 3d action representation learning. In *ACM MM*, 2021. 2, 3, 5, 6, 7
- [45] Zhigang Tu, Jiaxu Zhang, Hongyan Li, Yujin Chen, and Junsong Yuan. Joint-bone fusion graph convolutional network for semi-supervised skeleton action recognition. *IEEE TMM*, 2022. 2
- [46] He Wang, Feixiang He, Zhexi Peng, Tianjia Shao, Yongliang Yang, Kun Zhou, and David Hogg. Understanding the robustness of skeleton-based action recognition under adversarial attack. In *CVPR*, 2021. 2, 3
- [47] Peng Wang, Jun Wen, Chenyang Si, Yuntao Qian, and Liang Wang. Contrast-reconstruction representation learning for self-supervised skeleton-based action recognition. *IEEE TIP*, 31:6224–6238, 2022. 6
- [48] Qingtian Wang, Jianlin Peng, Shuze Shi, Tingxi Liu, Jiabin He, and Renliang Weng. Iip-transformer: Intra-inter-part transformer for skeleton-based action recognition. *arXiv*, 2021. 1
- [49] Shihao Xu, Haocong Rao, Xiping Hu, Jun Cheng, and Bin Hu. Prototypical contrast and reverse prediction: Unsupervised skeleton based action recognition. *IEEE TMM*, 25:624–634, 2021. 2, 6
- [50] Ziwei Xu, Xudong Shen, Yongkang Wong, and Mohan S Kankanhalli. Unsupervised motion representation learning with capsule autoencoders. In *NeurIPS*, 2021. 2
- [51] Sijie Yan, Yuanjun Xiong, and Dahua Lin. Spatial temporal graph convolutional networks for skeleton-based action recognition. In *AAAI*, 2018. 1, 6
- [52] Siyuan Yang, Jun Liu, Shijian Lu, Meng Hwa Er, and Alex C Kot. Skeleton cloud colorization for unsupervised 3d action representation learning. In *ICCV*, 2021. 2, 6
- [53] Han Yao, Sev-Jue Zhao, Chi Xie, Kenan Ye, and Shuang Liang. Recurrent graph convolutional autoencoder for unsupervised skeleton-based action recognition. In *ICME*, 2021. 2
- [54] Haoyuan Zhang, Yonghong Hou, Wenjing Zhang, and Wanqing Li. Contrastive positive mining for unsupervised 3d action representation learning. In *ECCV*, 2022. 2, 6
- [55] Jiahang Zhang, Lilang Lin, and Jiaying Liu. Hierarchical consistent contrastive learning for skeleton-based action recognition with growing augmentations. *arXiv*, 2022. 3, 4, 6, 7
- [56] Nenggan Zheng, Jun Wen, Risheng Liu, Liangqu Long, Jianhua Dai, and Zhefeng Gong. Unsupervised representation learning with long-term dynamics for skeleton based action recognition. In *AAAI*, 2018. 2, 6, 7